Digital Examination of Masonry Bridge Defects Using Point Cloud

Song Wu[1], Arijit Sen[1], Saeed Talebi[2]
[1]School of Architecture Design and Built Environment, Nottingham Trent University, Nottingham, UK
[2]School of Engineering & the Built Environment, Birmingham City University, Birmingham, UK.
Email: song.wu@ntu.ac.uk arijit.sen@ntu.ac.uk saeed.talebi@bcu.ac.uk

Abstract

There are significant numbers of masonry bridges on the U.K. railway network, which require regular condition monitoring by asset engineers and identify defects that would lead to structural failures. The most common defects observed in masonry structures are crack, spalling, bulging, joint defects, and loss of section. As a part of the bridge examination process, an engineer needs to be onsite, and sometimes it causes traffic interruption for a significant period to facilitate the examination process. Replacing the physical examination with a digital examination process would significantly reduce the number of site visits and traffic interruptions, which speed up the examination process and improve the safety and the efficiency of engineers' work. Point cloud data captured during the digital examination process has been successfully used in several studies to understand the accurate geometry of bridge structures, including detecting certain defects. Many software tools are available to perform the analysis on point cloud data. However, there is a gap in mapping and comparing the capabilities of that software in relation to the detection of masonry bridge defects. Therefore, this paper aims to analyse the ability of commonly used point cloud data analysis software to detect masonry defects in railway bridges.

Keywords: Digital Examination, Masonry Bridge Defects, Point Cloud Data Analysis, Defect Detection.

1. Introduction

Masonry bridges are a significant share of the U.K.'s transport network, and most of these bridges have been in operation for more than a century (McKibbins et al., 2006). The Railway network in the U.K. consists of approximately 18000 masonry bridges which are around 47% of its total bridge assets (Orbán, 2004). These bridges require regular monitoring by experienced engineers for the prevention of masonry defects to avoid any unexpected structural failures. The current examination practice requires a significant amount of planning, site visits, inspections and measurements of detected defects, and appropriate documentation by experts and engineers (Network Rail L3 / CIV / 006 Part 1B, 2019). The downside includes the closure of roads or lanes, which slow down the traffic flow, the expert and engineers need to travel to the site, and a large amount of manual input to prepare the documentation. As a result, a substantial amount of time is required to complete the whole process. The digital examination process refers to the capture of the entire physical asset with digital capture technology, such as Terrestrial Laser Scanning (TLS), or 360 imaging devices. Replacing physical examination with a digital examination process would considerably minimise some of these issues, for example, reducing the number of site visits by engineers and consequently shortening the overall examination time. There are other benefits of the digital examination process such as repeating an inspection with minimum effort, automated documentation at high level and quick validation of the examination report at different levels within the organisation. Terrestrial laser scanning and close-range photogrammetry (CRP) are the two standard procedures to generate digital 3D models of built environment. Terrestrial laser scanning is performed using a laser scanner that generates point cloud data as an output. CRP involves capturing a series of visual images from different angles and combine those images together to create a 3D model in the form of point cloud data (Luhmann et al., 2006). Point cloud data can convey important information about the actual geometry and surface condition of a scanned structure to a significant level of accuracy depending on the scan resolution. Study shows that measurement using point cloud data has achieved very close proximity with measurement using laser distometer (Kushwaha, Pande & Raghavendra, 2018). Both TLS and CRP are highly accurate in relation to size, shape and dimension of a

3D model; however, in a measurement study of vertical under clearance and beam geometry of bridges, TSL is found slightly ahead of CRP in terms of statistical correlation coefficient (Riveiro et al., 2013).

Significant research works have been conducted regarding the utilisation of point cloud data to monitor structural heath, identify common structural defects around the globe; and these research works have established the suitability of point could data in relation to structural defect detection (Rashidi et al., 2020). For example, Cavalagli et al. (2020) demonstrated the practicality of point cloud data analysis for detection of crack, material losses and spalling in a historical masonry bridge. Talebi et al. (2022) proposed a framework for digital inspection of railway bridges using point cloud data. Kushwaha et al. (2020) used TLS and CRP for generating point cloud data and achieved over 90% accuracy to classify areas with corrosion, vegetation, and water penetration in different bridge structures. In recent years, several researchers attempted to automatically identify and quantify crack, spalling and corrosion in concrete structures by analysing 2D image and point cloud data with the help of artificial neural network. For example, Yan et al., (2021) have demonstrated the use of convolutional neural network with visual (RGB) image and point cloud data to automatically detect and quantify crack on concrete structures, where more than 92% detection accuracy has been achieved. Peng et al. (2020) used high resolution 2D image and region based fully convolutional neural network to locate and classify the region of crack in concrete bridges. Wang et al. (2020) demonstrate a procedure to detect bridge bottom cracks in concrete structure using image stitching technique in 2D images which is captured using unmanned aerial vehicles (UAV). All these research works are limited to concrete structure only; and hence, there is a research scope to develop methodology for defect detection in masonry structures using point cloud data. The automated damage detection is still not reliable enough to be operated solely, rather it requires intervention and supervision from human experts (Dorafshan, Thomas & Maguire, 2018). Therefore, it is reasonable to primarily consider manual analysis of point cloud data with the help of commonly available software. Moreover, there are many software tools available to perform meaningful analysis on point cloud data including some effective and low-cost ones. As a result, systematic methods of point cloud data analysis have good potential to replace some elements of the physical examination process currently followed by rail engineers. This paper aims to investigate a digital analysis process through point could data for bridge examination. Point cloud data captured using TLS is considered for analysis in the current research. CloudCompare software is used to perform the analysis on point cloud data. CloudCompare is an open-source software with ability to efficiently analyse TLS point cloud data and it is widely used in several research in this field (Girardeau-montaut, 2016).

2. Masonry Defects

In general, masonry defects are categorised as bulging and leaning walls, failure in bonding and defects in joints, development of cracks, corrosion on the surfaces, defective cavity walls etc., (Noy & Douglas, 2005). However, masonry bridges do not have cavity walls and the defects observed are limited to bulging, crack, spalling and joints defect. According to Network Rail's L3/CIV/006 Part 1E, (2019) reference document, the masonry defects are classified as i) bulging, ii) crack/fracture/ring separation, iii) spalling, iv) joints defect and v) loss of section.

Table 1: Defect types and measurement requirements for different defects. (Source: Network Rail L3/CIV/006 Part 1E, 2019, pages 23-30)

Defect type	Measurement required for Severity extent							
	Area (m^2)	Length (mm)	Width (mm)	Aperture (mm)	Depth (mm)	Step (mm)	Distortion (degree)	Displacement (mm)
Bulging	Yes	Yes	Yes	No	No		Yes	No
Crack/ fracture/ ring separation	Yes	Yes	No	Yes	No	Yes	No	No
Spalling	Yes	Yes	Yes	No	Yes	No	No	No
Joint Defect	Yes	No	No	No	Yes	No	No	No
Loss of section	Yes	Yes	Yes	No	No	No	No	Yes

Each defect is further classified into several severity levels based on the dimension and location of the defects. As a result, it is required to measure specific dimensions for each defect during the examination process to evaluate the severity, the extent and the overall condition of a masonry bridge. To develop a method of point cloud data analysis for defect detection, it is necessary to understand the types of masonry defect and their inspection and measurement requirements. Table 1 represents the measurement requirements for each defect type in accordance with reference documents from Network Rail. It is found in Table 1 that three basic types of measurement are required to fulfil the examination criteria. These are:

i) area measurement to estimate the surface area covered by a particular defect,
ii) linear measurement such as length, width, depth, step, and aperture,
iii) angular measurement such as the magnitude of distortion.

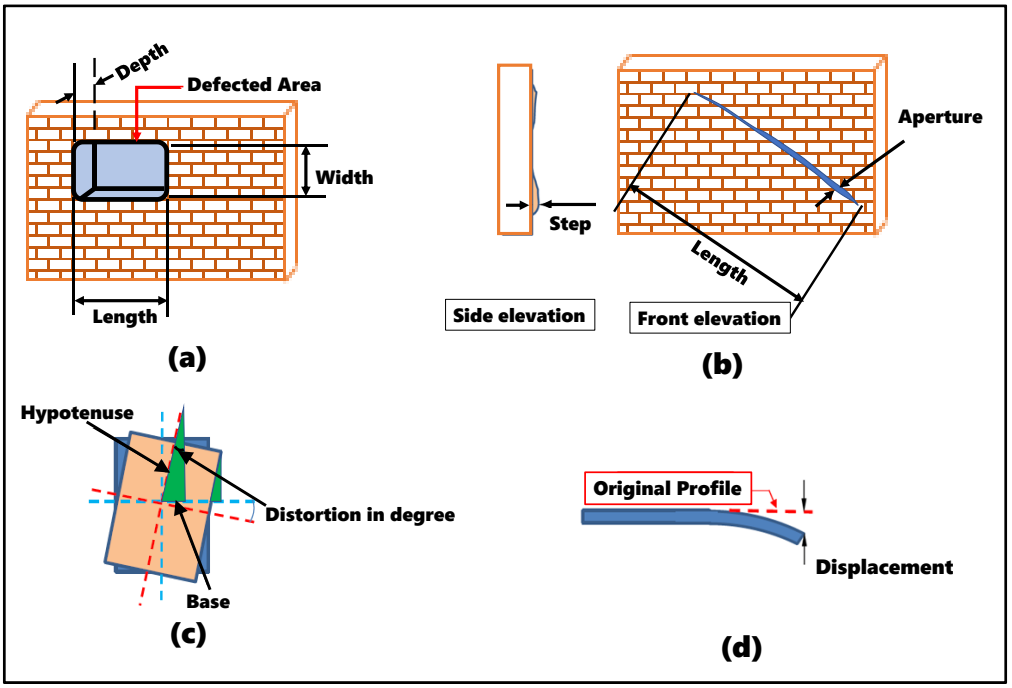

Figure 1: Understanding the measurement requirements for different defects.
Source: Network Rail L3/CIV/006 Part 1E, 2019.

Fig. 1-a schematically represents the length, width, and depth of a defect, as well as area covered by a defect such as spalling, joints defect etc. Fig. 1-b schematically shows the length of crack, step, and aperture of crack. Fig. 1-c shows a schematic representation of distortion in degree and Fig. 1-d schematically shows displacement. Distortion and displacement are required measurement criteria for bulging and loss of section respectively.

3. *Methodology*

The proposed methodology contains six steps which is presented in Fig. 2. It is assumed that the point could data is already registered, and geo-located.

Step 1: The registered point cloud data normally contains excess information in the form of noise such as data points that are not associated with the structure to be analysed. In this case, the surrounding environments including ground underneath a bridge are largely considered as noise. This information not only increases the file size of the point cloud dataset but also consumes high computing resources and computing time for performing analysis. As the purpose of the analysis is to look at the bridge defects only, the first step involves the removal of noise and surrounding environment from the registered point could data. It can be manually done with the help of segmentation tools available in most of the point cloud software. Some software provides automatic segmentation of surrounding environment to a certain extent; however, it requires manual intervention to precisely remove all noises.

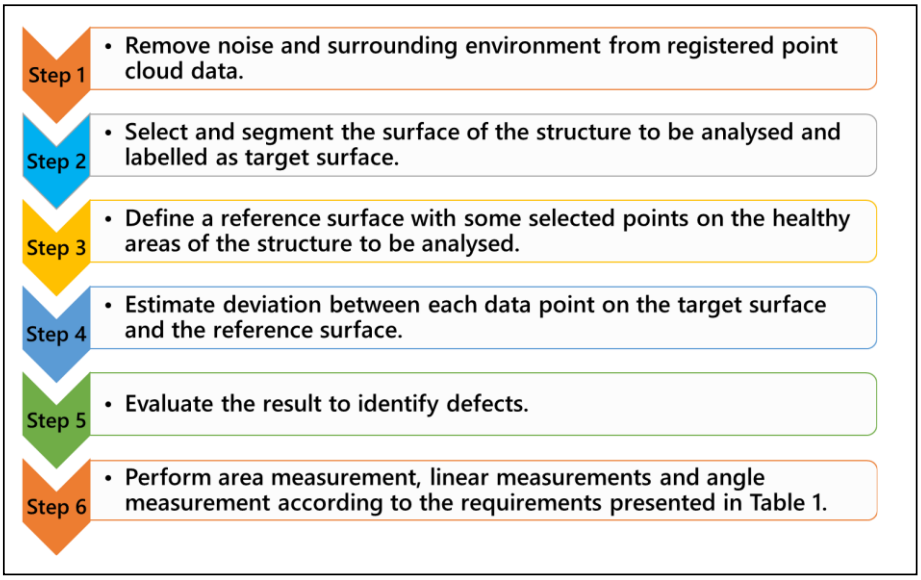

Figure 2: Flow chart of the proposed methodology.

Step 2: The key technique used for the analysis is to create a reference surface that represents a healthy state of the masonry structure and then estimate the deviation of point could data from the reference surface. Hence, it is required to select and segment the surface to be analysed and labelled as the target surface. The segmentation of the target surface from the whole structure will facilitate the analysis to be run on the target surface only. There are two benefits of it; firstly, it will not consider other surfaces on the structure which is less likely to provide any meaningful information; and secondly, it will expedite the overall analysis process. Moreover, previous research studies recommend segmentation of structures to be done prior to analysis for defect detection using digital techniques (Mirzazade et al., 2021; Riveiro, DeJong & Conde, 2016).

Step 3: To define the reference surface, some points on the healthy areas of the target surface are required to be selected. It is assumed that the healthy part of the surface represents an ideal surface which is defect free. Theoretically, the reference surface can be generated with a minimum of three points; however, taking more points would facilitate the generation of a highly accurate reference surface. Hence, it is recommended to pick as many points as possible on the healthy area to define the reference surface.

Step 4: This step involves the calculation of deviation between the reference surface and the target surface. Once the calculation is completed, the result is evaluated to detect the presence of defects. Most of the currently available software applications allow the user the perform linear distance calculations between a point cloud and a mesh surface. The current project uses CloudCompare software to perform the comparison. The software allows computing the signed distance between a reference mesh and a point cloud using Cloud-to-Mesh distance tool (Wiki, 2015).

Step 5: After completing the distance calculation, the result needs to be carefully evaluated to identify the presence of defects. A positive deviation from the reference plane represents the surface is coming out of its original position. This could happen either due to bulging if the deviation is observed over an area or due to the presence of cracks if the deviation is observed along a curve. A negative deviation from the reference surface is observed due to the presence of spalling, crack/fracture, joints defect or loss of section. The presence of a crack will show the deviation along a curve or line. The presence of joints defect will show the deviation along brick joints either as a straight line or as a stepped line. Loss of section will result in a negative deviation over an area. In general spalling also result in negative deviation; however, in some cases it could show a positive deviation if the spalled section tends to come out of a wall.

Step 6: This step involves performing required area measurements, linear measurements, and angle measurements for different defect types as presented in Table 1. CloudCompare software provides tools to measure any area bounded by a polyline and linear distance between two selected points. The

depth and step can be estimated by comparing the colour of the target surface, when presented using scaler intensity values, with the colour scale. Distortion can be estimated from the inverse sine formula as presented in equation (1) and according to the analogy presented in Fig. 1-c.

$$Distortion = \sin^{-1}\left[\frac{base}{hypotenuse}\right] \quad (1)$$

Here, hypotenuse represents the linear distance between a point on the healthy area and a point in area with the highest deviation on a target surface; base represents the numerical value of the highest deviation on any target surface as shown in Fig. 1-c.

4. *Result and Discussion*

The results of computed deviation between a reference surface and a target surface for different segments of a structure are presented in Fig. 3 to Fig. 6.

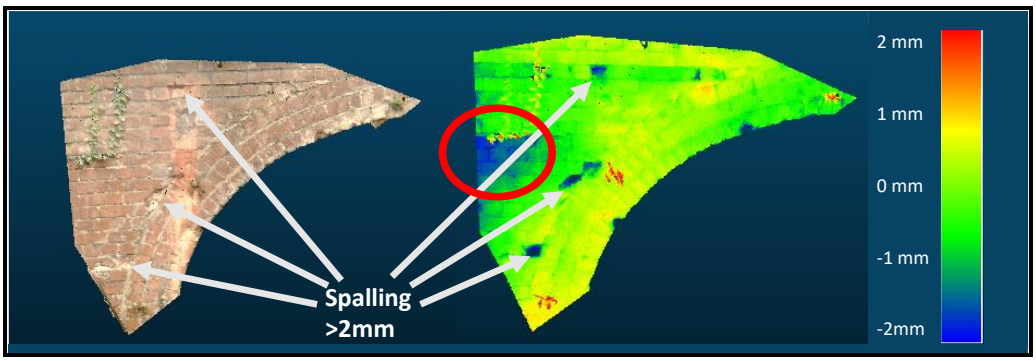

Figure 3: Detection of spalling >= 2mm.

Fig. 3 and Fig. 4 show examples of spalling detection using the proposed method at less than 2 mm depth and less than or equal to 5 mm depth, respectively. The visual image (on the left) in Fig. 3 shows the presence of spalling in three places and the scaler field presentation of the analysis result (on the right) shows the spalled area in blue colour which is pointed with arrows.

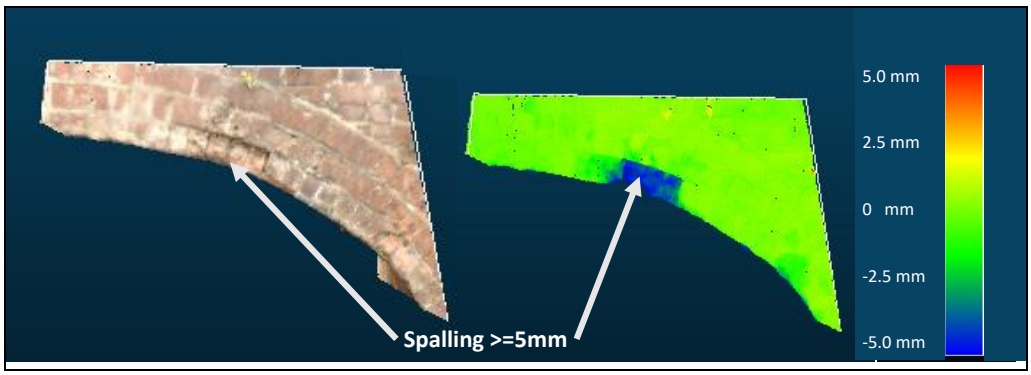

Figure 4: Detection of spalling >= 5mm.

It is noted from the colour bar [in Fig. 3] that the depth of spalling is nearly 2 mm for all three cases. A deformation in the wall is also noticed (circled in red) which is not possible to be detected from the visual image. The red areas on the scaler field image show the presence of vegetation although it is not taken into consideration at this point. Similarly, Fig. 4 shows the presence of spalling with a depth around 5 mm. Fig. 5 presents examples of crack detection and joints defect detection using the proposed method. In the visual image at the top left of Fig. 5, window A shows the presence of crack and window B shows the presence of joints defects. The scalar field representation of the analysis result at the bottom right shows the corresponding areas of crack and joints defect. Fig. 6 shows an example of bulging detection using the proposed method. The surface analysis performed on the right side wall of the arch reveals the presence of irregularities on the wall surface. The blue areas represent the wall deviated inward by 20 mm and the red areas represent the wall deviated outward by 20 mm. The outward deviation is considered as bulging.

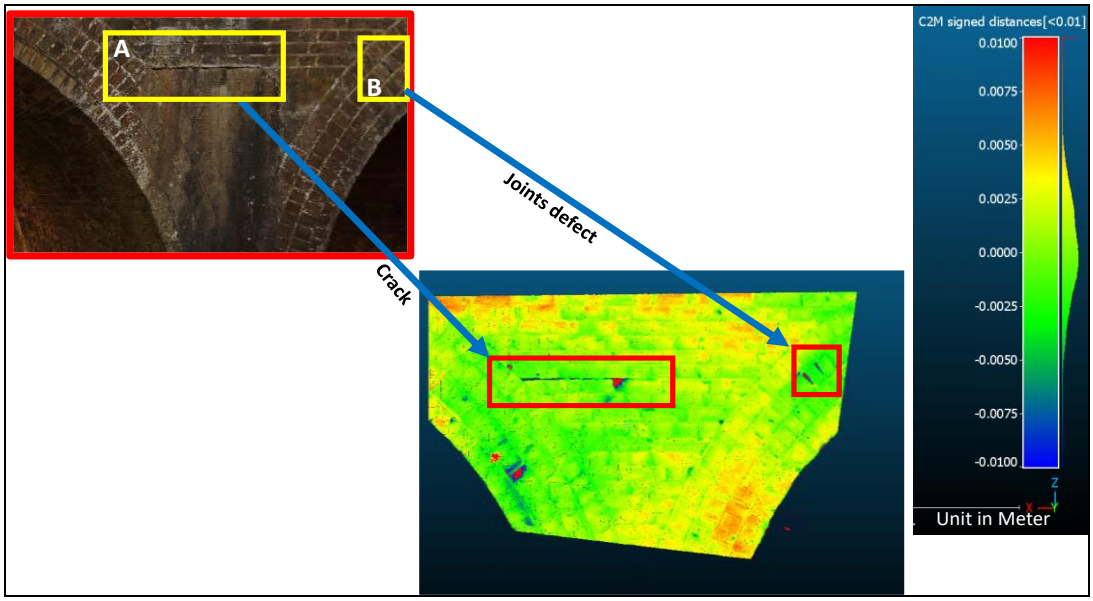

Figure 5: Detection of crack and joints defect.

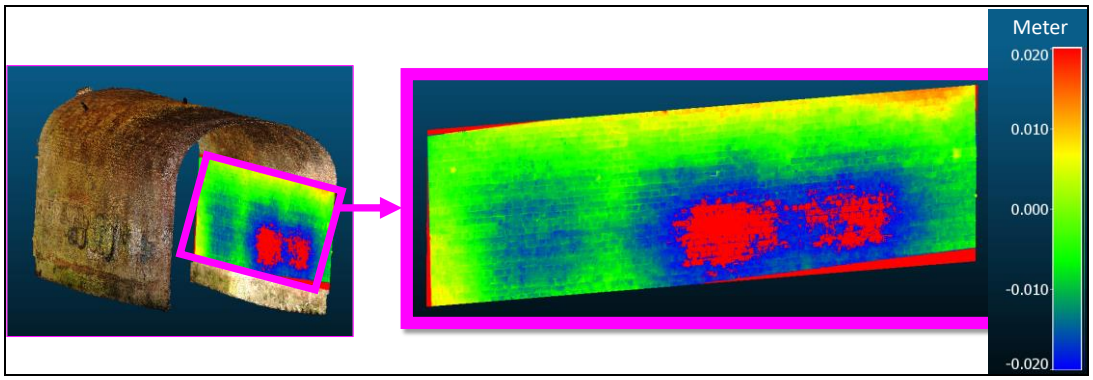

Figure 6: Detection of bulging.

The examples of measurement techniques discussed in step 6 of the methodology section are shown in Fig. 7 to Fig. 11. In CouldCompare, measurement of any area covered with a defect can be performed by bounding that area with a polyline and extracting the estimated area from its property pane. The software facilitates the estimation of an area with any shape; and hence, the area of complex shapes can be precisely measured which is difficult to achieve in physical measurements.

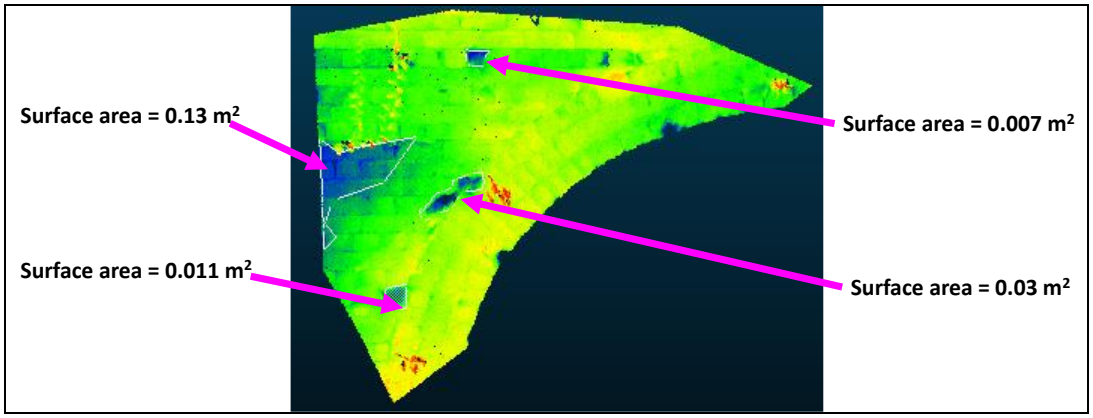

Figure 7: Measurement of area for spalling.

Fig. 7 shows examples of surface area measurement of complex shapes on the target surface that is identified as spalling. The linear measurement of depth, step and displacement can be achieved from the colour bar associated with the scaler filed representations [Fig. 3 - Fig. 6].

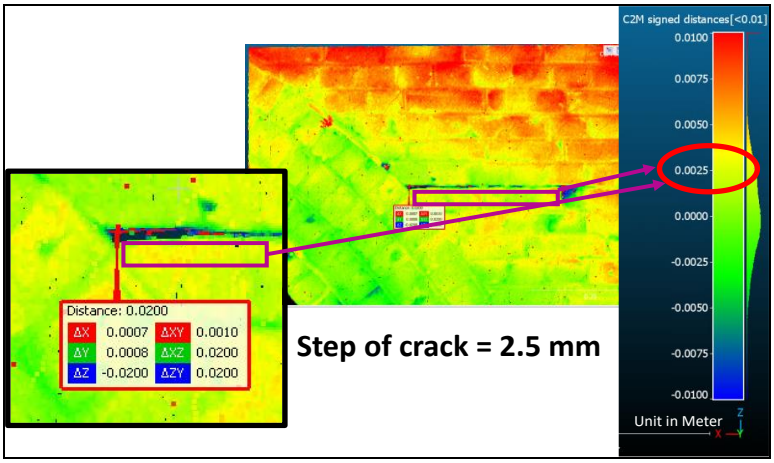

Figure 8: Measurement of step for crack.

Fig. 8 shows an example of a step measurement for a detected crack. From the colour bar associated with the scaler intensity image of the analysis result the estimated step is around 2.5 mm. Linear distance measurement between two selected points can be implemented for the measurement of length, width, and aperture. CloudCompare software has a tool that allows users to estimate the distance between any two picked points (Girardeau-Montaut, 2015).

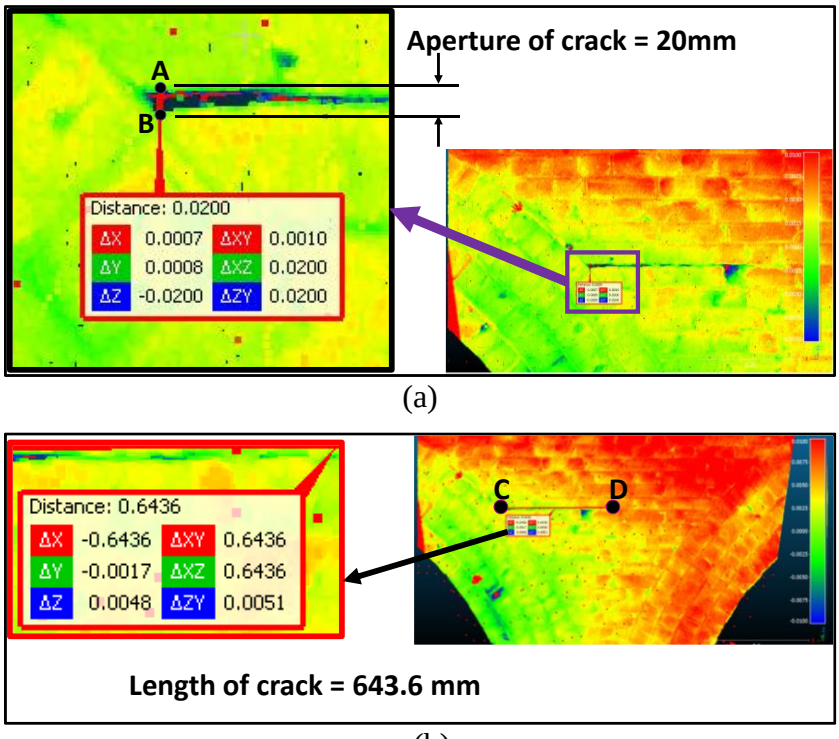

Figure 9: (a) Measurement of aperture for crack, (b) Measurement of crack length.

Fig. 9-a shows an example of aperture measurement for a crack where the aperture is the linear distance between points A and B. using the point picking tool in CloudCompare the aperture is measured as 20 mm. Fig. 9-b shows an example of determining the length of crack using point picking tool in terms of the linear distance between two points C and D which is 643.6 mm. It is noticed from both figures that in addition to the linear distance in 3D space, the point picking tool also provides the difference between the points in all three axes in the form of ΔX, ΔY and ΔZ all three planes in the form of ΔX.Y., ΔY.Z. and ΔX.Z. Therefore, measurement should be carefully performed by taking the appropriate 3D distance. The distortion measurement for bulging requires some additional calculation

using equation (1). The hypotenuse can be estimated by picking one point in the healthy area and other points on the area with the highest deviation from the reference surface.

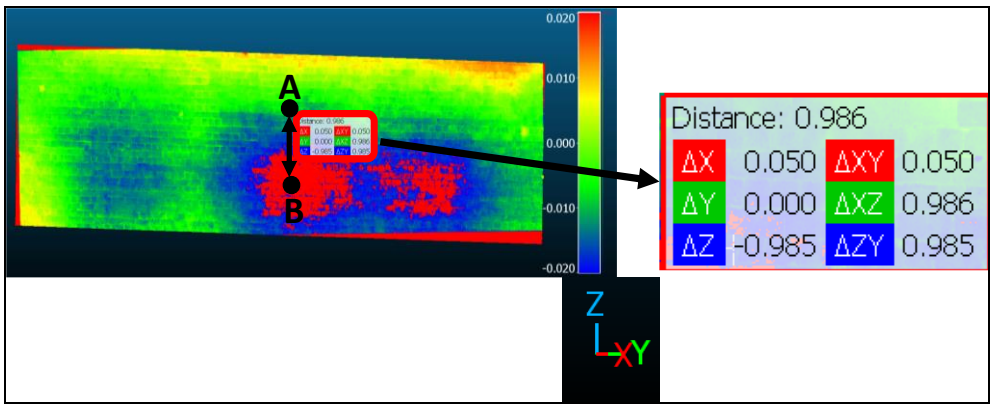

Figure 10: Measurement of bulging.

In Fig. 10, point A represents a point on the healthy surface and point B represents a point on the area with the highest deviation from the reference surface. The distance between these points is measured in the same way as it is done for length and aperture measurements, and it is found to be 986 mm in this case. The base in equation (1) is the value of deviation at point B which is estimated as 20 mm with the help of the colour bar as shown in Fig. 6. Replacing these values in equation (1), the distortion is calculated as 1.17°.

5. *Conclusion*

Switching from physical examination to digital examination for maintenance of masonry bridges would enhance the accuracy of the examination process, shorten the time required and reduce the cost associated with the examination process. Point cloud data obtained from 3D scanning using TLS has been largely used in the civil engineering domain to enhance the accuracy of a structure's geometric information. Literature shows that significant research has been conducted for defect detection in concrete structures. However, limited study has been carried out in masonry structures. A sequential analysis method is developed for the identification and measurement of masonry defects in railway bridges using point cloud data to satisfy the examination requirements for bridge examination. The implementation of the proposed method for the analysis of four different defect types has been demonstrated. The result established the feasibility of implementing point cloud data analysis techniques for masonry defect detection and measurement. It also shows the practicability of using point cloud data to perform required measurement for the bridge examination process. Detection and measurement for loss of section are not demonstrated in the current paper due to the absence of the defect in the available data set. However, it is expected that the proposed method can be successfully implemented for detection and measurement of loss of section as well because it is similar to the detection procedure of spalling. The current analysis process involves the manual execution of different steps using CloudCompare software. Future research will focus on the ability of other popular point cloud software to perform similar steps as well as the possibility of automation to facilitate the rapid execution of the examination process.

Acknowledgements

The research is supported by the Network Rail under Shift2Rail programme, In2Track3 project. The contents of this publication are the sole responsibility of its authors and cannot be taken to reflect the views of Network Rail. Point cloud data obtained from In2Track2 project of Network Rail under Shift2Rail programme is used in this paper.

References

Cavalagli, N. et al., 2020. On the accuracy of UAV photogrammetric survey for the evaluation of historic masonry structural damages. *Procedia Structural Integrity*, 29, pp. 165–174. doi:10.1016/j.prostr.2020.11.153.

Dorafshan, S., Thomas, R.J. & Maguire, M., 2018. Fatigue Crack Detection Using Unmanned Aerial Systems in Fracture Critical Inspection of Steel Bridges. *Journal of Bridge Engineering*, 23(10), p. 040180781-0401807815. doi:10.1061/(ASCE)BE.1943-5592.0001291.

Girardeau-montaut, D., 2016. CloudCompare, *in France: EDF R&D Telecom ParisTech*, 11. Available at: http://pcp2019.ifp.uni-stuttgart.de/presentations/04-CloudCompare_PCP_2019_public.pdf (Accessed: 30 June 2022).

Girardeau-Montaut, D., 2015. CloudCompare version 2.6.1, user manual. Available at: http://www.danielgm.net/cc/ (Accessed: 7 March 2022).

Kushwaha, S.K.P. et al., 2020. Analysis and Integration of Surface and Subsurface Information of Different Bridges. *Journal of the Indian Society of Remote Sensing*, 48(2), pp. 315–331. doi:10.1007/s12524-019-01087-2.

Kushwaha, S.K.P., Pande, H. & Raghavendra, S., 2018. Digital Documentation, Bridge Deck Linearity Deformation and Deck Thickness Measurement Using Terrestrial Laser Scanner (TLS) and Close Range Photogrammetry (CRP). *ISPRS Annals of the Photogrammetry, Remote Sensing and Spatial Information Sciences*, IV–5(5), pp. 47–51. doi:10.5194/isprs-annals-IV-5-47-2018.

Luhmann, T. et al., 2006. Close Range Photogrammetry: Principles, Techniques and Applications. 1st edn. Scotland: Whittles Publishing. Available at: https://www.researchgate.net/publication/237045019_Close_Range_Photogrammetry_Principles_Techniques_and_Applications (Accessed: 18 June 2022)..

McKibbins, L.D. et al, 2006. Masonry arch bridges : condition appraisal and remedial treatment. CIRIA C656. London: CIRIA publication. Available at: https://www.networkrail.co.uk/wp-content/uploads/2017/02/CIRIA-report-Masonry-arch-bridges-condition-appraisal-and-remedial-treatment.pdf (Accessed: 18 June 2022).

Mirzazade, A. et al., 2021. Workflow for Off-Site Bridge Inspection Using Automatic Damage Detection-Case Study of the Pahtajokk Bridge. *Remote Sensing*, 13(14), p. 2665. doi:10.3390/rs13142665.

Network Rail L3 / CIV / 006 Part 1B, 2019. NR / L3 / CIV / 006 Part 1B Undertake Examinations, pp. 1–26.

Network Rail L3 / CIV / 006 Part 1E, 2019. NR / L3 / CIV / 006 Part 1E Structures Defects, pp. 23–30.

Noy, E.A. & Douglas, J., 2005. Building Surveys and Reports. 3rd edn. Edited by M. Malden. Oxford: Blackwell Publication.

Orbán, Z., 2004. Assessment, reliability and maintenance of masonry arch railway bridges in Europe. *Proceedings of 4th International Conference on Arch Bridges*, *Barcelona*, (152–161), pp. 1–10. Available at: http://arch-bridges.fzu.edu.cn/html/Conference/2015/07/13/cdb34f28-0084-4749-8007-3550ef61cc90.html.

Peng, X. et al., 2020. The Feasibility Assessment Study of Bridge Crack Width Recognition in Images Based on Special Inspection UAV. *Advances in Civil Engineering. Edited by X. Fan*, 2020, pp. 1–17. doi:10.1155/2020/8811649.

Rashidi, M. et al., 2020. A decade of modern bridge monitoring using terrestrial laser scanning: Review and future directions. *Remote Sensing*, 12(22), pp. 1–34. doi:10.3390/rs12223796.

Riveiro, B. et al., 2013. Validation of terrestrial laser scanning and photogrammetry techniques for the measurement of vertical underclearance and beam geometry in structural inspection of bridges. *Measurement*, 46(1), pp. 784–794. doi:10.1016/j.measurement.2012.09.018.

Talebi, S. et al., 2022. The development of a digitally enhanced visual inspection framework for masonry bridges in the UK. *Construction Innovation*, 22(3), pp. 624–646. doi:10.1108/CI-10-2021-0201.

Wang, H.F. et al., 2020. Measurement for cracks at the bottom of bridges based on tethered creeping unmanned aerial vehicle. *Automation in Construction*, 119(February 2019), p. 1-13. doi:10.1016/j.autcon.2020.103330.

Wiki, C. (2015) Cloud-to-Mesh Distance. Available at: https://www.cloudcompare.org/doc/wiki/index.php?title=Cloud-to-Mesh_Distance (Accessed: 20 June 2022).

Yan, Y. et al. (2021) 'Towards automated detection and quantification of concrete cracks using integrated images and lidar data from unmanned aerial vehicles', Structural Control and Health Monitoring. doi:10.1002/stc.2757.